

# Preparation and Characterization of Homogeneous Hydroxyapatite/Chitosan Composite Scaffolds via *In-Situ* Hydration

Hong Li<sup>1,2\*</sup>, Chang-Ren Zhou<sup>1,2</sup>, Min-Ying Zhu<sup>1</sup>, Jin-Huan Tian<sup>1,2</sup>, Jian-Hua Rong<sup>1,2</sup>

<sup>1</sup>Department of Materials Science and Engineering, Jinan University, Guangzhou, China; <sup>2</sup>Education Ministry Research Centre of Artificial Organs & Materials, Jinan University, Guangzhou, China.  
Email: \*tlihong@jnu.edu.cn, hli2@clemsun.edu

Received May 14<sup>th</sup>, 2010; revised June 5<sup>th</sup>, 2010; accepted June 30<sup>th</sup>, 2010.

## ABSTRACT

Hydroxyapatite(HAP)/Chitosan(CS) composite is a biocompatible and bioactive material for tissue engineering. A novel homogeneous HAP/CS composite scaffold was developed via lyophilization and *in situ* hydration. A model CS solution with a Ca/P atom ratio of 1.67 was prepared through titration and stirring so as to attain a homogeneous dispersion of HAP particles. After lyophilization and *in situ* hydration, rod-shaped HAP particles (5  $\mu\text{m}$  in diameter) within the CS matrix homogeneously scattered at the pore wall of the CS scaffold. X-ray diffraction (XRD) and Fourier-Transformed Infrared spectroscopy (FTIR) confirmed the formation of HAP crystals. The compressive strength in the composite scaffold indicated a significant increment over a CS-only scaffold. Bioactivity *in vitro* was completed by immersing the scaffold in simulated body fluid (SBF), and the result suggested that there was an increase in apatite formation on the HAP/CS scaffolds. Biological *in vivo* cell culture with MC 3T3-E1 cells for up to 7 days demonstrated that a homogeneous incorporation of HAP particles into CS scaffold led to higher cell viability compared to that of the pure CS scaffold or the HAP/CS scaffold blended. The results suggest that the homogeneous composite scaffold with better strength, bioactivity and biocompatibility can be prepared via *in vitro* hydration, which may serve as a good scaffold for bone tissue engineering.

**Keywords:** Hydroxyapatite, Chitosan, Scaffold, Composite, Hydration

## 1. Introduction

Tissue engineering, which applies methods from engineering and life sciences to create artificial constructs to direct tissue regeneration, has attracted many scientists and surgeons with a hope to treat patients in a minimally invasive and less painful way. The important process of a tissue engineering paradigm is to isolate specific cells to grow them on a scaffold. A scaffold should be in combination with support for tissue architecture, biomolecules and selective transportation of ions in body fluids. Chitosan (CS) is the partially deacetylated form of chitin that can be extracted from crustacean. Apart from being bioresorbable, it is biocompatible, non-harmful, non-toxic compounds and biofunctional. In addition, CS is easy to mould a 3-dimensional scaffold which can support tissue ingrowth, aid in the formation of tissue structure, and promote growth and mineral rich matrix deposition by osteoblast in culture for bone tissue engineering [1]. It is

important to note that CS in combination with hydroxyapatite (HAP,  $\text{Ca}_{10}(\text{PO}_4)_6(\text{OH})_2$ ), further enhance tissue regenerative efficacy and osteoconductivity [2-4]. HAP can accelerate the formation of bone-like apatite on the surface of implant and can induce bone formation [5]. By the way, incorporation of HAP into a CS polymer matrix has also been shown a significant enhancement of mechanical strength [6].

Several studies have focused on the composite scaffold for bone tissue engineering [7-9], such as CS/calcium phosphate [7], CS/HAP bilayer scaffold [8]. The composite had been prepared by different processing, such as mechanical mixing of HAP powder in a solution [10,11], co-precipitation [12], and biomimetic process [13,14]. Generally, HAP powder was mixed with CS dissolved in 2% acetic acid solution, poured into a mould, and freezing-dried to make sponge composites. The final material was heterogeneous, which was shown in the macroscopically less homogeneous. However, to ensure a more

effective contact between scaffold and tissue, a homogeneous composite scaffold should be prepared. In addition, a uniform distribution of inorganic particles in polymer matrix theoretically and experimentally improves mechanical property [15,16].

The present work aims to design and develop a homogeneous composite scaffold fabricated from biopolymer CS and bioceramic HAP as a candidate for bone tissue engineering applications. It is hypothesized that a homogeneous HAP dispersion could lead to an enhancement on mechanically competent, bioactivity and biocompatibility. Generally, a homogeneous dispersion can be obtained if the materials mixed and formed in an aqueous environment. However, CS is acid-soluble while HAP usually forms in a solution with  $\text{pH} > 10$ . Therefore, in order to achieve a homogeneous HAP/CS composite scaffold, the combination of the lyophilization method and *in situ* hydration in alkaline aqueous was applied in this work. The composition, morphology, mechanical property, bioactivity and biocompatibility of the homogeneous composite scaffold were studied.

## 2. Experimental Procedures

### 2.1. Preparation of the Composite Scaffold

CS powder was supplied commercially with the degree of deacetylation over 97% (Shanghai Boao Biotechnology Co., Shanghai, China; the viscosity-average relative molecular weight was  $1.8 \times 10^6$  Da.). A CS aqueous solution of 2 wt% was prepared by dissolving CS powder into deionized water containing 2 wt% acetic acid. Then, under agitation, a stoichiometric 2 mol/L  $\text{CaCl}_2$  solution was slowly added into the CS solution. Subsequently, a 1.2 mol/L  $\text{K}_2\text{HPO}_4$  solution, with a Ca/P atom ratio of 1.67, was added dropwise. The ratio of HAP to CS solution was 60/100 by weight. After stirring, the suspension was put into dishes (diameter of 30 mm, and depth of 5 mm) and 24-well plates (diameter of 14 mm, and depth of 14 mm), and then rapidly transferred into a freezer at presented temperature  $-40^\circ\text{C}$  to solidify the water and induced phase separation. The solidifying route maintained at that temperature over night. In the next stage, frozen samples were lyophilized using a freeze-dryer (Uniequip, Germany) for 24 hrs. The obtained scaffolds were hydrated with a mixture of 0.1 N sodium hydroxide solution and pure ethanol with a 2:1 volumetric ratio for different time periods. After *in situ* hydration, the samples washed with deionized water till the pH of washout water was about 7. Finally, the samples treated were freeze-dried again to obtain the CS/HAP porous scaffolds. The samples were denoted by D.

As a control, HAP/CS composite scaffold was prepared via blending method. Briefly, HAP powder (Boao

Bio. Tech. Com., Shanghai, China) was added into a CS aqueous solution of 2 wt% acetic acid (HAP/CS solution is 60/100, wt/wt) with magnetic stirring and ultrasonic treatment. After stirring, the mixture was moulded, frozen and lyophilized as described above. The samples were denoted by E, while the pure CS scaffold was denoted by A.

### 2.2. SEM Examination

The lyophilized scaffolds were cut with a razor blade to expose the inner surfaces. After being coated with gold in a sputtering device, the samples were examined with a scanning electron microscope (XL-30 ESEM, Philips Co., Netherland) with an accelerating voltage of 20 kV.

### 2.3. XRD

The composite scaffold samples were ground to fine powder after frozen in liquid  $\text{N}_2$  for 30 minutes, and then characterized by X-rays diffraction (XRD; MASL, Beijing, China, 40 kV, 20 mA,  $3^\circ/\text{min}$ ).

### 2.4. FTIR

The HAP/CS scaffolds prepared via lyophilization and *in situ* hydration were analyzed by Fourier-transform infrared attenuated total reflective spectroscopy (FT-IR; EQUINOX 55, Bruker, Germany). The scaffolds were frozen in liquid  $\text{N}_2$  for 30 minutes and were ground into a fine powder. The powder samples were mixed with KBr powder and compressed into pellets for FT-IR examination. The spectra were collected over the range of  $4000\text{-}400\text{ cm}^{-1}$ .

### 2.5. Compressive Strength Measurement

The samples of each of the three type scaffolds (A, CS-only; D, HAP/CS composite *in situ* hydrated; E: HAP/CS composite blended) were cut into rectangle ( $5.0\text{ mm} \times 5.0\text{ mm} \times 5.0\text{ mm}$ ). The compressive strength was measured using a computer-controlled Universal Testing Machine (AG-1, Shimadzu Co., Tokyo, Japan) with a guideline set in ASTM D5024-95a. The strength was calculated by using the yield point load divided by the specimen's cross sectional area. Five parallel samples were evaluated for each of the scaffolds.

### 2.6. Incubation in Simulated Body Fluid (SBF)

To evaluate the bioactivity of the composite scaffolds *in vitro*, the samples were incubated in SBF (the prescription of SBF referring to Ref. [17]). The 1 g samples were placed into SBF (50 ml) and incubated at  $37^\circ\text{C}$ . The concentrations of Ca and P ions in SBF were measured at 1, 3 and 7 days incubation by inductively coupled plasma atomic emission spectrometry (Optima 2000 DV, Perkin

Elmer Co., USA). Morphologies of the incubated scaffolds were observed by SEM as described before.

## 2.7. Cell Culture

Osteoblast Cells line MC 3T3-E1 (a clonal preosteoblastic cell line derived from newborn mouse calvaria, which is often used in bone tissue engineering research) were cultured in DMEM supplemented with 10% fetal bovine serum (GIBCO Co., U.S.A.), 100 U/mL penicillin (Sigma, St. Louis, MO), and 100 µg/mL streptomycin (Sigma). Cells were incubated at 37°C in a 5% CO<sub>2</sub> incubator, and the medium was changed every 2 days. When the cells reached the stage of confluence, they were harvested by trypsinization followed by the addition of fresh culture medium to create a cell suspension. A cell suspension with a concentration of  $2 \times 10^6$  cells/mL was loaded into the 3-D porous scaffolds (14 mm in diameter and 2 mm in thickness), with 200 µL of suspension for each scaffold. The scaffolds were put in a polystyrene 24-well flat-bottom culture plate and incubated at 37°C in a 5% CO<sub>2</sub> incubator. After cells attached at about 6 hrs, fresh culture medium was added until the total medium volume was 500 µL. Culture medium was changed every 2 days.

## 2.8. Cell Viability Assessment

A MTT assay was applied in this study to quantitatively assess the number of viable cells attached and grown on the tested scaffolds. Briefly, all the tested scaffolds with cultured cells at predetermined time points were fetched to a new 24-well flat-bottom culture plate. 1 mL of serum-free medium and 100 µL of MTT (Sigma) solution (5 mg/mL in PBS) were added to each sample, followed by incubation at 37°C for 4 h for MTT formazan formation. The upper solvent was removed and 1 mL of 10% sodium dodecyl sulfate (Sigma) in 0.01N HCl was added to dissolve the formazan crystals for 6 h at 37°C. During the dissolving period, the spongy scaffolds were squeezed every 30 min to ensure the complete extraction of the formazan crystals. The optical density (OD) at 490 nm was determined against the sodium dodecyl sulfate solution blank. Five parallel replicates were analyzed for each sample.

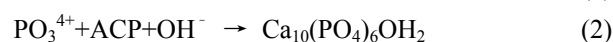
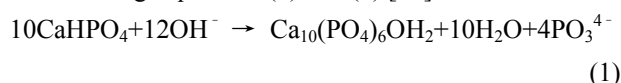
## 3. Results and Discussion

### 3.1. Phase Analysis

The XRD patterns of the D sample before and after hydration for different hydration periods are summarized in **Figure 1**. The XRD patterns were verified by the Power Diffraction File (HAP: Card No. 090432; CS: Card No. 391894; DCPD: No. 720713; KCl: No. 730713). It indi-

cated that, the DCPD and KCl crystalline phases mainly occurred in the scaffolds D before hydration. The longer the hydration ripening time, the smoother the peaks belong to DCPD and KCl. After 24 h of ripening, DCPD and KCl crystalline phases disappeared in the composite scaffold D. The broad peak that appeared around 20° was assigned to CS (20.305°, 21.290°), and the sharp diffraction characteristic peaks that appeared at around 31.8° and 25.9° correspond to the peaks of HAP (31.773°, 25.879°).

For pH of HAP formation more than 10, it was observed that DCPD (brushite), and (or) amorphous CaP occurred when Ca<sup>2+</sup> and HPO<sub>4</sub><sup>2-</sup> were directly dropped into a CS solution with pH < 7 (**Figure 1(b)**). During the process of *in situ* hydration in the mixture solution of sodium hydroxide solution and pure ethanol, the unstable brushite, as well as the other amorphous CaP phases transformed into a more stable HAP phase, according to the following Equations (1) and (2) [18].



As Pang's report [19] and our study, after 24 h of ripening, the transformation of brushite and amorphous CaP to HAP was found nearly completely.

XRD patterns show the presence of KCl in the CS composite before hydration due to the precipitation of KCl during the lyophilization. After the composites were hydrated and washed, KCl solved and disappeared as indicated in **Figure 1**.

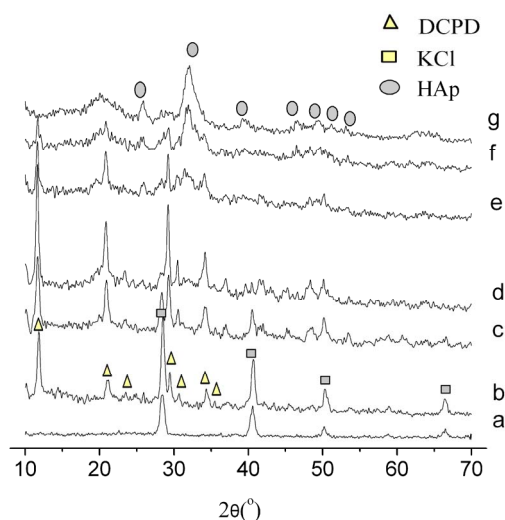


**Figure 1.** XRD patterns of (a) KCl, HAP/CS composite scaffold D before hydration (b), after 1 hr (c), after 3 hrs (d), after 6 hrs (e), 12 hrs (f) and 24 hrs (g) hydration.

### 3.2. FTIR

An infrared absorption spectra of the scaffold is summarized in **Figure 2**. The absorption bands at  $3540\text{ cm}^{-1}$ ,  $3487\text{ cm}^{-1}$  and  $633\text{ cm}^{-1}$  respectively correspond to the stretching and vibration of the lattice  $\text{OH}^-$  ions, while the bands of absorbed water are shown at  $3287\text{ cm}^{-1}$ ,  $3163\text{ cm}^{-1}$ ,  $1648\text{ cm}^{-1}$ . The characteristic bands for  $\text{HPO}_4^{2-}$  were assigned at  $1133\text{ cm}^{-1}$ ,  $1064\text{ cm}^{-1}$ ,  $989\text{ cm}^{-1}$ ,  $875\text{ cm}^{-1}$ ,  $577\text{ cm}^{-1}$ ,  $527\text{ cm}^{-1}$  [20]. The magnitude of these bands became weaker with the development of *in situ* hydration and finally disappeared. The characteristic bands for  $\text{PO}_4^{3-}$  appeared at  $963\text{ cm}^{-1}$  for the  $\nu_1$  mode [21-22]. The signal became clearly as the hydration processing. The observation of the  $\nu_3$  symmetric P-O stretching vibration at  $1032/1042\text{ cm}^{-1}$  as a distinguishable peak, together with the bands  $566/602\text{ cm}^{-1}$  corresponding to  $\nu_4$  bending vibration indicates the presence of HAP in the samples as summarized in **Figure 2(c, d, e, f, g, h)**. These peaks show obviously stronger after 24 hours ripening, in accord with the XRD results.

### 3.3. Morphology Analysis

The morphologies of the scaffolds were examined with SEM. The CS-only scaffold A, composite scaffold D after hydration showed a similar spongy appearance (**Figure 3**) in macroscopic morphology, which indicated that both adding the HAP in the system and hydrating the scaffolds did not influence the porous structure. Due to the artifact of the sample preparation for SEM, the pores

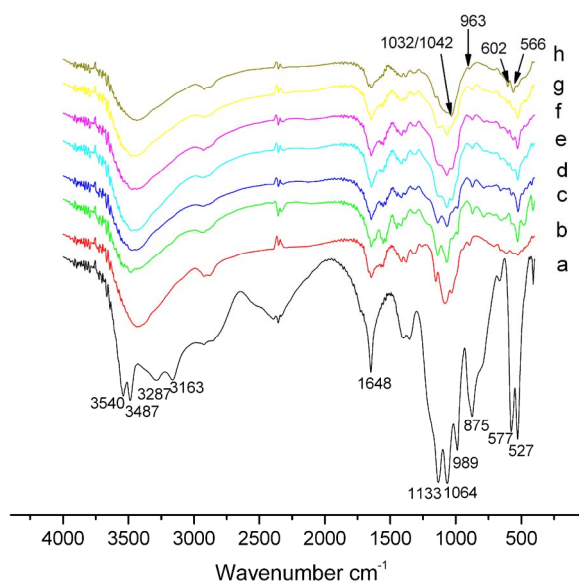


**Figure 2.** IR spectra of DCPD (a), CS (b), composite scaffold D before hydration (c), after 1 hr (d), after 3 hrs (e), after 6 hrs (f), 12 hrs (g) and 24 hrs (h) hydration.

in the A scaffold were collapsed as illustrated in **Figure 3(a)**. The D scaffolds depict more regular porous structure (**Figure 3(e)**), for its relative high strength can resist the distortion during the sample preparation. However, the microscopic morphology on pore-wall surfaces was quite different. The surface of the scaffold A is smooth as shown in **Figure 3(b)**. Before hydration processing was applied, the walls of D are embedded with flower-shaped large particles, as indicated in **Figures 3(c) and (d)**. After hydration, the rod like HAP particles with about  $5\text{ }\mu\text{m}$  in diameter were homogeneously scattered in the pore-wall surfaces of the composite scaffold D as shown in **Figure 3(f)**. The SEM results suggest that HAP particles can be homogeneously incorporated with CS matrix via lyophilization and *in situ* hydration process.

### 3.4. Mechanical Property

The compressive strength of A, D and E are illustrated in the **Figure 4**. Sample D has the highest compressive strength when compared to the control. Li reported that the incorporation HAP into CS matrix via blending method would result in the decrease of mechanical properties of HAP/CS material due to the weaker interfacial bonding between HAP filler and CS matrix [23]. However, in our study, no obvious decrease appeared in aspect of mechanical property blended HAP/CS sponge E.

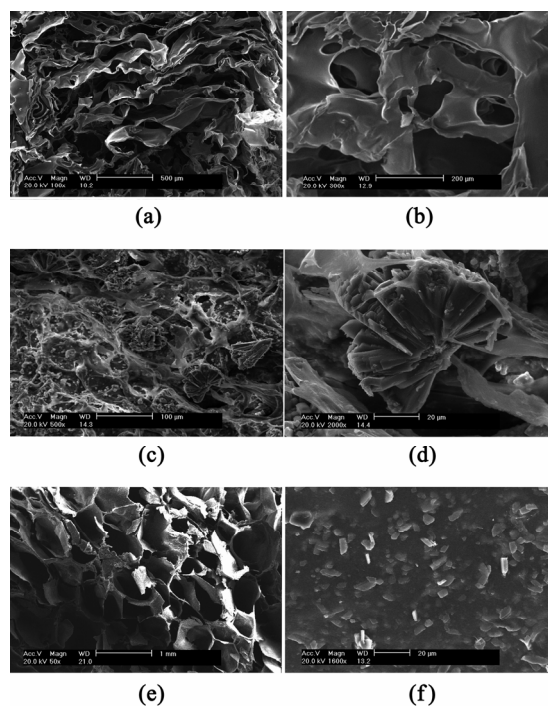


**Figure 3.** SEM morphologies of CS-only scaffold (a), the pore wall of the CS-only scaffold (b), composite scaffold D before hydration(c)(d) and after hydration (e)(f).

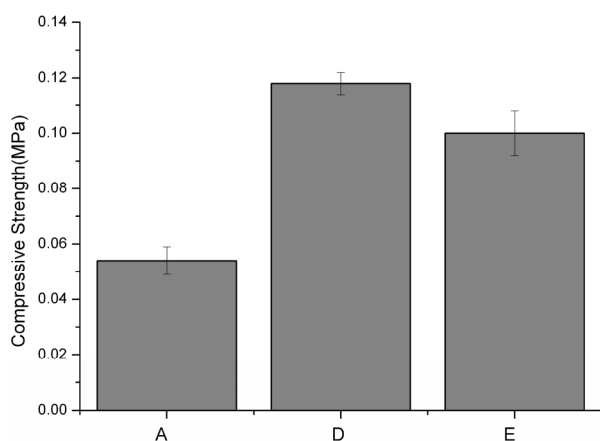


**Figure 4.** Compressive strength of the scaffolds A, D after 24 hrs hydration and composite via blending E. Data represented the mean  $\pm$  SD for five samples.  $p < 0.01$  compared with pure CS.

The composite scaffold D prepared by *in situ* hydration, with HAP particles homogeneously dispersion, has a little increment in compressive strength and less derivation, as compared to the control E. The compressive strength indicated that the observed homogeneous particle dispersion would be helpful to enhance the scaffold mechanically competent.

### 3.5. Bioactivity

According to Kokubo *et al.*, the *in vitro* immersion of bioactive materials in SBF was thought to reproduce *in vivo* surface structures [13,24,25]. The grown layer is sometimes called a bone-like apatite [25]. A bone-like apatite layer plays an important role in establishing the bone-bonding interface between biomaterials and living tissue [4]. As shown in **Figure 5**, the surface of the soaked scaffolds in SBF showed spherical particles containing tiny crystals which correspond to apatite [26-28]. The size and number of the apatite particles formed on the D scaffold was obviously larger than those of the particles on the scaffolds A and E. The apatite crystals on the sample D also depict a relatively uniformly size according **Figure 5**, unlike those on the sample E that larger particles occurred. With the immersion periods going, the quantities of apatite particles increased in macroscopic morphology, but the difference still existed. The scaffolds A and E were covered with tiny apatite crystals while some larger particles dotted on the E scaffold, but a layer of particle crystals fully covered the wall of the D scaffold. This result is also supported by the results of the Ca and P concentration decrease in SBF.

**Figure 6** displays the concentrates of Ca and P ions in SBF, which soaked the samples. An abrupt decrease in

the concentrates of Ca and P ions during the first three days followed by a continuous slow decrease in the next days. The result is in agreement with the SEM observation for changes in macroscopic morphologies after the first three days. This appreciable decrease in Ca and P concentrations can be attributed to the formation of apatite crystals on the specimen surfaces. However, the decreases of Ca and P concentrations in the SBF, which the composite scaffolds D and E were soaked, were larger than that of scaffold A. It is just confirmed that the amount of apatite formed on the scaffold A was less than that of apatite on the composite scaffolds D and E as shown in **Figure 5**. The large apatite crystals dotted on the scaffold E also led to the decrease in the concentrations of Ca and P ions more rapidly than that of scaffold D in the first three day.

According to **Figure 6**, as a result of the difference of crystallinity of HAP, a little increase of Ca and P concentrates at the first day in **Figure 6** D sample is shown. The HAP particles synthesized at low temperatures have been shown to have low crystallinity and high solubility [29]. Therefore, the poorly crystallized HAP in the D scaffolds formed via *in situ* hydration within the solution has high solubility, which led to ions release in the SBF media at early time. There was an increment in the concentration of both Ca and P ions after 12 hrs immersion of the scaffold D in SBF. In the scaffold A, the increment of Ca and P concentrates might be the de-chelate release of CS-Ca chelate at neural environment.

Despite the difference of HAP particles, the scaffolds with HAP (D and E) still show better bioactivity as compared to the CS scaffold A when the scaffolds were soaked in SBF. HAP would be favor to the nucleation of bone-like apatite for HAP particles could act as nucleation sites in a metastable calcium phosphate solution

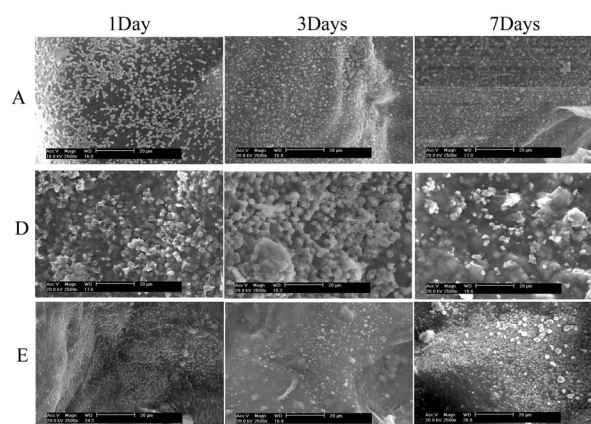


**Figure 5.** SEM morphologies of the pore walls of the samples A, composite D after 24 hrs hydration and composite via blending E in SBF after 1, 3 and 7 days immersion.

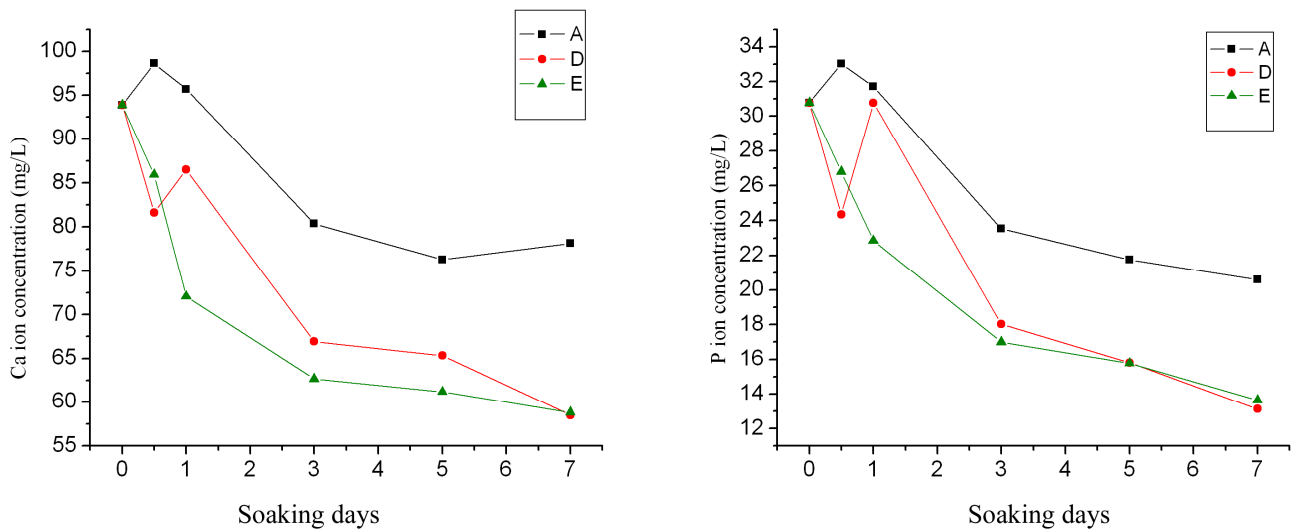


**Figure 6.** Concentrations of Ca ions (a) and P ions (b) in SBF in which the samples were immersed (A. CS-only; D. composite D after 24 hrs hydration; E. composite via blending).

such as SBF [30]. However, a homogeneous dispersion of HAP in composite can obviously induced a homogeneous precipitation of bone-like apatite in SBF, and would be improve the bioactivity more effectively.

### 3.6. Cell Test

The biocompatibility of the scaffolds A, D and E was assessed on cells' proliferation. Cell proliferation was examined with MTT assay (Figure 7). The same amount of MC 3T3-E1 cells were seeded on the scaffolds A, D and E. MC 3T3-E1 is a preosteoblast cell line derived

from newborn mouse calvaria, which usually is used to evaluate the biocompatibility of the materials for bone tissue engineering. At early 3 day time, a MTT value of sample A has the highest one. After 7 days' culture, the value of the D scaffold was the higher than the others scaffolds, which indicated that the MC 3T3-E1 cells showed much better viability property on D. It is an indication of both the process and the component of HAP might have significant difference in some degree on the biocompatibility of these scaffold materials.

### 4. Conclusions

In this paper, a homogeneous HAP/CS composite scaffold was prepared and investigated. HAP particles were combined homogeneously with CS matrix through lyophilization and *in situ* hydration in alkaline solution. As compared to the controls, the composite scaffold indicated an increment in mechanical strength, altogether with a homogeneous bone-like apatite precipitation in SBF. The difference processing for fabricating the CS/HAP composite scaffold also showed significant difference in cell's biocompatibility according to this study. The results on the homogeneous composite indicate that this novel process is a new approach to fabricating bone tissue engineering scaffolds especially for composite scaffold. Further reports about *in vivo* study will be reported in the near future.

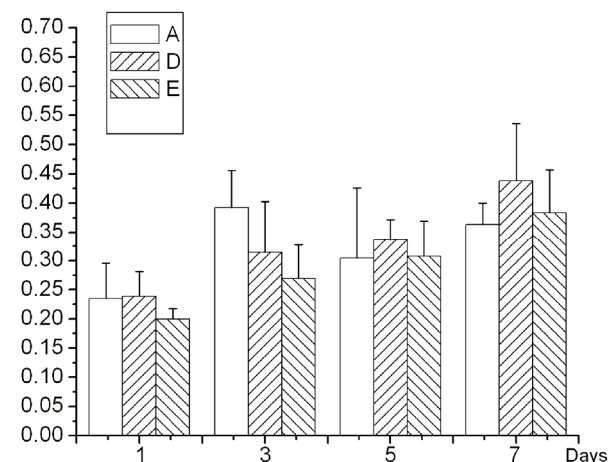


**Figure 7.** MTT assay of cells grown on CS scaffold and composite porous scaffolds. Data represent the mean  $\pm$  SD for three samples.  $p < 0.01$  compared with pure CS. (A: CS-only; D: composite D after 24 hrs hydration; E: composite via blending).

### 5. Acknowledgements

The authors wish to thank the National High Technology Development Program of China (2007AA091603) and the National Science Foundation of China (30870612,

20604010) for supporting this research.

## REFERENCES

- [1] Y. J. Seol, J. Y. Lee, Y. J. Park, Y. M. Lee, Y. Ku, I. C. Rhyu, S. J. Lee, S. B. Han and C. P. Chung, "Chitosan Sponges as Tissue Engineering Scaffolds for Bone Formation," *Biotechnology Letters*, Vol. 26, No. 13, 2004, pp. 1037-1041.
- [2] F. Zhao, W. L. Grayson, T. Ma, B. Bunnell and W. W. Lu, "Effects of Hydroxyapatite in 3-D Chitosan-Gelatin Polymer Network on Human Mesenchymal Stem Cell Construct Development," *Biomaterials*, Vol. 27, No. 9, 2006, pp. 1859-1867.
- [3] T. Kawakami, M. Antoh, H. Hasegawa, T. Yamagishi, M. Ito and S. Eda, "Experimental Study on Osteoconductive Properties of a Chitosan-Bonded Hydroxyapatite Self-Hardening Paste," *Biomaterials*, Vol. 13, 1992, pp. 759-763.
- [4] Z. Ge, S. Baguenard, L. Y. Lim, A. Wee and E. Khor, "Hydroxyapatite-Chitin Materials as Potential Tissue Engineered Bone Substitutes," *Biomaterials*, Vol. 25, No. 6, 2004, pp. 1049-1058.
- [5] L. J. Kong, Y. Gao, G. Y. Lu, Y. D. Gong, N. M. Zhao and X. F. A. Zhang, "Study on the Bioactivity of Chitosan/Nano-Hydroxyapatite Composite Scaffolds for Bone Tissue Engineering," *European Polymer Journal*, Vol. 42, No. 12, 2006, pp. 3171-3179.
- [6] Q. Hu, B. Li, M. Wang and J. Shen, "Preparation and Characterization of Biodegradable Chitosan/Hydroxyapatite Nanocomposite Rods via in Situ Hybridization: A Potential Material as Internal Fixation of Bone Fracture," *Biomaterials*, Vol. 25, No. 5, 2004, pp. 779-785.
- [7] Y. Zhang and M. Zhang, "Synthesis and Characterization of Macroporous Chitosan/Calcium Phosphate Composite Scaffolds for Tissue Engineering," *The Journal of Biomedical Materials Research*, Vol. 55, No. 3, 2001, pp. 304-312.
- [8] J. M. Oliveira, M. T. Rodrigues, S. S. Silva, P. B. Malafaya, M. E. Gomes, C. A. Viegas, I. R. Dias, J. T. Azevedo, J. F. Mano and R. L. Reis, "Novel Hydroxyapatite/Chitosan Bilayered Scaffold for Osteochondral Tissue-Engineering Applications: Scaffold Design and its Performance When Seeded with Goat Bone Marrow Stromal Cells," *Biomaterials*, Vol. 27, 2006, pp. 6123-6137.
- [9] S. Viala, M. Freche and J. L. Lacout, "Preparation of a New Organic Mineral-Composite: Chitosan-Hydroxyapatite," *Annals of Chemical-Science of Materials*, Vol. 23, 1998, pp. 69-72.
- [10] F. Zhao, Y. Yin, W. W. Lu, J. C. Leong, W. Zhang, J. Zhang, M. Zhang and K. Yao, "Preparation and Histological Evaluation of Biomimetic Three-Dimensional Hydroxyapatite/Chitosan-Gelatin Network Composite Scaffolds," *Biomaterials*, Vol. 23, 2002, pp. 3227-3234.
- [11] M. V. Correlo, F. B. Luciano, B. Mrinal, F. M. Joao, M. N. Nuno and L. R. Ruis, "Hydroxyapatite Reinforced Chitosan and Polyester Blends for Biomedical Applications," *Macromolecular Materials and Engineering*, Vol. 290, 2005, pp. 1157-1165.
- [12] X. Shen, H. Tong, T. Jiang, Z. Zhu, P. Wan and J. Hu, "Homogeneous Chitosan/Carbonate Apatite/Citric Acid Nano-Composites Prepared through a Novel in Situ Precipitation Method," *Journal of Computer Science and Technology*, Vol. 67, No. 11-12, 2007, pp. 2238-2245.
- [13] T. Kokubo, M. Hanakawab, M. Kawashita, Minoda, T. Beppu, T. Miyamoto and T. Nakamura, "Apatite Formation on Non-Woven Fabric of Carboxymethylated Chitin in SBF," *Biomaterials*, Vol. 25, No. 18, 2004, pp. 4485-4488.
- [14] K. Tuzlakoglu and R. L. Reis, "Formation of Bone-Like Apatite Layer on Chitosan Fiber Mesh Scaffolds by a Biomimetic Spraying Process," *Journal of Materials Science: Materials in Medicine*, Vol. 18, No. 7, 2007, pp. 1279-1286.
- [15] Z. H. Guo, S. Y. Wei, B. Shedd, R. Scaffaro, T. Pereira and H. T. Hahn, "Particle Surface Engineering Effect on the Mechanical, Optical and Photoluminescent Properties of ZnO/Vinyl-Ester Resin Nanocomposites," *Journal of Materials Chemical*, Vol. 17, 2007, pp. 806-813.
- [16] M. C. Kuo, C. Tsai, J. C. Huang, M. Chen, "PEEK Composites Reinforced by Nano-Sized SiO<sub>2</sub> and Al<sub>2</sub>O<sub>3</sub> Particulates," *Materials Chemistry and Physics*, Vol. 90, No. 1, 2005, pp. 185-195.
- [17] T. Kokubo, H. Kushitani, C. Ohtsuki, S. Sakka and T. Yamamuro, "Chemical Reaction of Bioactive Glass and Glass-Ceramics with a Simulated Body Fluid," *Journal of Materials Science: Materials in Medicine*, Vol. 1, 1992, pp. 79-83.
- [18] V. M. Rusua, C. H. Ng, M. Wilke, B. Tierscha, P. Fratzl and M. G. Peter, "Size-Controlled Hydroxyapatite Nanoparticles as Self-Organized Organic-Inorganic Composite Materials," *Biomaterials*, Vol. 26, No. 26, 2005, pp. 5414-5426.
- [19] Y. X. Pang and X. Bao, "Influence of Temperature, Ripening Time and Calcination on the Morphology and Crystallinity of Hydroxyapatite Nanoparticles," *Journal of European Ceramic Society*, Vol. 23, No. 10, 2003, pp. 1697-1704.
- [20] T. K. Anee, M. Palanichamy and M. Ashok, "Influence of Iron and Temperature on the Crystallization of Calcium Phosphates at the Physiological pH," *Materials Letters*, Vol. 58, No. 3, 2004, pp. 478-482.
- [21] C. W. Chen, R. E. Riman, K. S. Tenhuisen and K. Brown, "Mechanochemical-Hydrothermal Synthesis of Hydroxyapatite from Nonionic Surfactant Emulsion Precursors," *Journal of Cryst Growth*, Vol. 270, No. 3-4, 2004, pp. 615-623.
- [22] G. C. Koumoulidis, A. P. Katsoulidis, A. K. Ladavos, P. J. Pomonis, C. C. Trapalis, A. T. Sdoukos and T. C. Vaimakis, "Preparation of Hydroxyapatite via Microemulsion Route," *Journal of Colloid and Interface*

- Science*, Vol. 259, 2003, pp. 254-260.
- [23] B. Q. Li, Q. L. Hu, X. Z. Qian, Z. P. Fang and J. C. Shen, "Bioabsorbable Chitosan/Hydroxyapatite Composite Rod for Internal Fixation of Bone Fracture Prepared by in Situ Precipitation," *Acta Polymerica Sinica*, Vol. 6, 2002, pp. 828-833.
- [24] T. Kokubo, I. Ito and T. Huang, "P-Rich Layer Formed on High-Strength Bioactive Glass-Ceramics A-W," *Journal of Biomedical Materials Research*, Vol. 24, 1990, pp. 331- 343.
- [25] P. Li, C. Ohtsuki and T. Kokubo, "Effects of Ions in Aqueous Media on Hydroxyapatite Induction by Silica Gel and Its Relevance to Bioactivity of Bioactive Glasses and Glass/ Ceramics," *Journal of Applied Biomaterials*, Vol. 4, 1993, No. 3, pp. 221-229.
- [26] A. S. Posner, "The Mineral of Bone," *Clinical Orthopaedics Related Research*, Vol. 200, 1985, pp. 87-93.
- [27] T. Kokubo, "Apatite Formation on Surfaces of Ceramics, Metals and Polymers in Body Environment," *Acta Materialia*, Vol. 46, No. 7, 1998, pp. 2519-2527.
- [28] X. Lu and Y. Leng, "Theoretical Analysis of Calcium Phosphate Precipitation in Simulated Body Fluid," *Biomaterials*, Vol. 26, No. 10, 2005, 1097-1108.
- [29] T. Matsumoto, M. Okazaki, M. Inoue, S. Yamaguchi, T. Kusunose, T. Toyonaga, Y. Hamada and J. Takahashi, "Hydroxyapatite Particles as a Controlled Release Carrier of Protein," *Biomaterials*, Vol. 25, No. 17, 2004, pp. 3807-3812.
- [30] T. Kokubo, "Apatite Formation on Surfaces of Ceramics, Metals and Polymers in Body Environment," *Acta Materialia*, Vol. 46, No. 7, 1998, pp. 2519-2527.